

# Structure–Dynamics Relationships in Random Poly(butylene isophthalate-*co*-butylene adipate) Copolyesters As Revealed by Dielectric Loss Spectroscopy and X-ray Scattering

C. Alvarez,<sup>†</sup> M. J. Capitan,<sup>†</sup> N. Lotti,<sup>‡</sup> A. Munari,<sup>‡</sup> and T. A. Ezquerra<sup>\*,†</sup>

*Instituto de Estructura de la Materia, C.S.I.C., Serrano 119, Madrid 28006, Spain, and Dipartimento di Chimica Applicata e Scienza dei Materiali, Università di Bologna, Via Risorgimento 2, 40136 Bologna, Italy*

*Received December 20, 2002; Revised Manuscript Received February 10, 2003*

**ABSTRACT:** The structure–dynamics relationships in random copolymers of poly(butylene adipate) and poly(butylene isophthalate) (PBIPBA) have been investigated by means of X-ray scattering and dielectric loss spectroscopy experiments. The results show that the incorporation of flexible butylene adipate units into the more rigid PBI chain increases the ability to crystallize the resulting copolymer as compared to that of PBI. The subglass dynamics of the copolymers is characterized by the existence of two processes,  $\beta'$  and  $\beta''$  assigned to the relaxation of the individual butylene adipate (BA) and butylene isophthalate (BI) comonomeric units, respectively. The  $\beta''$ -relaxation of the amorphous specimens exhibits an unexpected enhanced mobility with increasing BA molar ratio, which has been explained by considering a progressive increase of the intrachain cooperativity. The segmental dynamics for the amorphous specimens, characterized by the  $\alpha$ -relaxation, follows an expected molar ratio behavior. However, an anomalous effect characterized by an enhancement of the segmental mobility induced by the crystallinity is observed in the 50/50 copolymer. This effect has been explained by considering the progressive enrichment of the amorphous phase in butylene adipate segments as crystallinity develops.

## 1. Introduction

The physical properties of random copolymers strongly depend on composition and physical properties of the individual homopolymers. Additionally, if both homopolymers are capable of crystallizing, the corresponding random copolymers are likely to develop crystallinity or not mainly depending on the nature of the comonomeric units, composition, and thermal treatment. Similar to what happens in homopolymers,<sup>1,2</sup> the molecular motions occurring in the amorphous phase of copolymers are strongly affected by the degree of crystallinity.<sup>3</sup> In semicrystalline random copolymers at temperatures higher than the glass transition temperature,  $T_g$ , the amorphous copolymer segments are confined to relax among crystalline regions. This restriction may strongly modify the relaxation behavior of the copolymer and affect the different mechanisms for energy dissipation in the system. As a consequence, crucial physical properties like toughness, strength, and mechanical stability, among others, are affected by the crystallinity. For this reason it seems necessary to seek for particular structure–dynamics relationships in random copolymers in order to be able to control the physical properties in an optimal way. In recent years, random copolyesters are gaining industrial relevance mainly due to the possibility of tailoring the thermal and dynamical behavior. Particularly, random copolymers of poly(butylene adipate) (PBA) and poly(butylene isophthalate) (PBI) are of potential interest as low melting temperature thermoplastics with adhesive properties. These materials are frequently referred to as “hot melts”. The two constituent homopolymers present very different physical properties. PBA is a very flexible,  $T_g = -63$  °C, and highly crystalline,<sup>4</sup> whereas PBI is more rigid,<sup>5</sup>  $T_g = 23$  °C. The crystallization behavior of poly-

(butylene isophthalate-*co*-butylene adipate) (PBIPBA) copolyesters was found to be strongly dependent on molar ratio.<sup>6</sup> Although the thermal<sup>7</sup> and dilute solution properties<sup>8</sup> of PBIPBA random copolyesters have been investigated, not so much attention has been devoted neither to the study of the relaxation behavior nor to the possible relations between dynamics and structure.

The aim of the present work is to establish, for this copolymeric system, relationships between the relaxation behavior, as characterized by dielectric loss spectroscopy, and the degree of ordering, as revealed by X-ray scattering methods.

## 2. Experimental Part

Poly(butylene isophthalate) (PBI), poly(butylene adipate) (PBA), and poly(butylene isophthalate-*co*-butylene adipate) copolymers (PBIPBA) of various compositions were synthesized according to the well-known two-stage polycondensation procedure described elsewhere.<sup>8</sup> Both molecular and thermal characterization data<sup>7,8</sup> are collected in Table 1. Figure 1 represents the chemical structure of the counts.

Complex dielectric permittivity measurements ( $\epsilon^* = \epsilon' - i\epsilon''$ ) were performed over a frequency range of  $10^{-1} < F < 10^6$  Hz in a temperature range of  $-150$  °C  $< T < T_g + 70$  °C. A Novocontrol (Huntsangen, Germany) system integrating an ALPHA dielectric interface was employed. The temperature was controlled by means of a nitrogen gas jet (QUATRO from Novocontrol) with a temperature error of  $\pm 0.1$  during every single sweep in frequency. The samples were prepared by melt pressing between two aluminum electrodes (20 mm in diameter) separated by 0.12 mm thick Kapton spacers<sup>9</sup> followed by a fast quenching on ice–water. The Kapton spacers were used in order to control the sample thickness and to avoid short-circuit of the two electrodes. This procedure produced amorphous specimens of PBI, 20PBIPBA, and 50PBIPBA and semicrystalline 20PBIPBA and PBA. Semicrystalline 80PBIPBA and 50PBIPBA samples were prepared from the amorphous ones, keeping them at room temperature for 1 week. To obtain semicrystalline PBI, the sample was kept in a furnace for 24 h at 126 °C in accordance with a previous

<sup>†</sup> Instituto de Estructura de la Materia, C.S.I.C.

<sup>‡</sup> Università di Bologna.

**Table 1. Molecular, Thermal, and Structural Characterization Data for PBA, PBI, and PBIPBA Copolymers with Different BI/BA Molar Ratio<sup>a</sup>**

sample	mole ratio BI/BA	$10^{-3}\bar{M}_n$	$T_g^b$ (°C)	$T_m$ (°C)	$X_c$	$L$ (nm)
PBI	100/0	13.0	23	145		
80PBIPBA	80/20	11.7	5	115	0.11	9.8
50PBIPBA	50/50	8.9	-25	64	0.10	14.1
20PBIPBA	20/80	9.7	-48	47	0.20	19.2
PBA	0/100	7.3	-63 <sup>c</sup>	64	0.51	11.7

<sup>a</sup> Number-average molar masses ( $\bar{M}_n$ ), glass transition temperature ( $T_g$ ), melting temperature ( $T_m$ ) were taken from refs 7 and 8. Degree of crystallinity ( $X_c$ ) and long space ( $L$ ) were estimated for samples crystallized at room temperature for 1 week. <sup>b</sup> Data referring to totally amorphous samples. <sup>c</sup> Value obtained by extrapolation of the experimental copolymer  $T_g$  data.

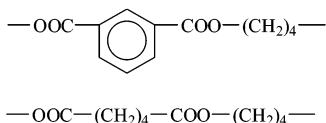


**Figure 1.** Chemical structure of the counits involved in the PBIPBA random copolymers investigated: butylene isophthalate (BI) (top); butylene adipate (BA) (bottom).

published procedure.<sup>5</sup> The dielectric relaxations were empirical described in terms of the Havriliak–Negami (HN) equation:

$$\epsilon^* = \epsilon_\infty + \frac{\epsilon_0 - \epsilon_\infty}{[1 + (i\omega\tau)^b]^c} \quad (1)$$

where  $\epsilon_0$  and  $\epsilon_\infty$  are the relaxed ( $\omega = 0$ ) and unrelaxed ( $\omega = \infty$ ) dielectric constant values,  $\tau$  is the central relaxation time of the relaxation time distribution function, and  $b$  and  $c$  ( $0 < b, c < 1$ ) are shape parameters which describe the symmetric and the asymmetric broadening of the relaxation time distribution function, respectively.<sup>10</sup> An additional contribution of the conductivity process was taken into account by adding a term  $-i(\sigma/(\epsilon_{\text{vac}}\omega))^s$  to eq 1. Conductivity is usually associated with generation and transport of polarization-induced charges through the polymer under the action of an electric field. Here  $\sigma$  is related to the direct current electrical conductivity,  $\epsilon_{\text{vac}}$  is the dielectric constant of vacuum, and the value of the coefficient  $0 < s < 1$  depends on the conduction mechanism.<sup>11</sup> Wide-angle X-ray scattering (WAXS) experiments were conducted at room temperature by means of a Seifert (XRD 3000) symmetrical reflection  $\theta/2\theta$  scanning diffractometer with Ni-filtered Cu K $\alpha$  wavelength. The goniometer geometry was set with the Si(111) Bragg peak. The instrumental resolution was  $\Delta s = 8.3 \times 10^{-4} \text{ \AA}^{-1}$ . The instrumental background was subtracted. A crystallinity index,  $X_c^{\text{WAXS}}$ , was calculated as the ratio between the integrated area below the crystalline peaks to the total experimental scattered integral intensity. It was considered the deconvoluted crystalline contribution, given by the crystal reflections, and the amorphous one, which is present in the form of an amorphous halo.<sup>12</sup> The error in the crystallinity index was evaluated as  $\pm X_c \cdot 0.1$ , which mainly appears from the limitation of the covered angular range. Small-angle X-ray scattering (SAXS) experiments were performed at room temperature by using synchrotron radiation in the Soft Condensed Matter beamline A2 at HASYLAB (DESY) synchrotron facility in Hamburg (Germany). A X-ray wavelength  $\lambda = 0.15 \text{ nm}$  was employed. Angular calibration for SAXS experiments was accomplished by using a collagen sample from a rat tail. Each frame was collected for 60 s and later corrected for primary beam intensity fluctuations during experiment and background.<sup>13</sup>

### 3. Results

**3.1. X-ray Scattering Experiments.** Figure 2 illustrates the WAXS patterns at room temperature of the PBIPBA samples as a function of the scattering

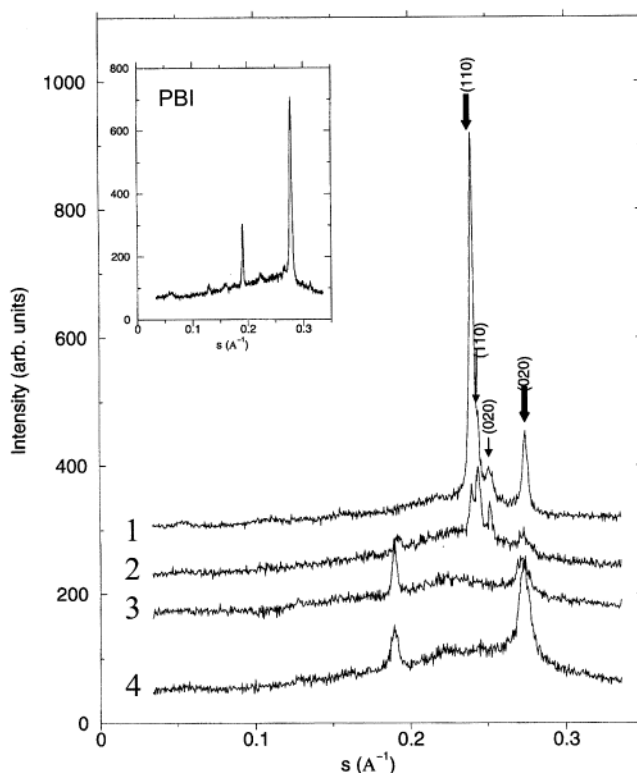


**Figure 2.** WAXS diffracted intensity as a function of reciprocal lattice vector  $s = (2/\lambda) \sin(\theta)$ ,  $2\theta$  being the scattering angle, for the investigated semicrystalline copolymers: (1) PBA, (2) 20PBIPBA, (3) 50PBIPBA, (4) 80PBIPBA. Arrows for PBA indicate spacings corresponding to the PBA crystalline phases reported. Inset shows the diffraction pattern of semicrystalline PBI.

vector  $s$ , where  $s = (2/\lambda) \sin \theta$ ,  $2\theta$  being the scattering angle, performed after a week of holding time at ambient conditions following the preparation of the film. PBI does not crystallize under this condition due to its  $T_g$  value.<sup>6</sup> To obtain information about the crystalline structure of PBI, this sample was crystallized at 126 °C for 24 h. The corresponding WAXS pattern is presented as inset in Figure 2. All samples present Bragg peaks characteristic of a crystalline structure. The estimates for the crystallinity index,  $X_c^{\text{WAXS}}$ , are given in Table 1. The position of the Bragg peaks for PBI (inset of Figure 2) appears located at 0.060, 0.129, 0.158, 0.190, 0.223, 0.266, 0.278, 0.298, and 0.312  $\text{\AA}^{-1}$ , in agreement with previously reported X-ray patterns.<sup>5</sup> The WAXS patterns of the PBIPBA copolymers are formed by diffraction peaks which are essentially in the same position with respect to those present in the X-ray spectrum of PBI. In particular, the most intense Bragg peaks, around  $s = 0.19$  and  $0.27 \text{ \AA}^{-1}$ , characteristic of the PBI homopolymer,<sup>5</sup> are detected even in the sample containing the lowest amount of butylene isophthalate units (20PBIPBA). However, a slight shift in the spacings of the Bragg peaks as the BI/BA molar ratio is varied suggests the possibility that a small amount of butylene adipate units are partially introduced as defects in the crystalline structure of PBI. The WAXS pattern of PBA exhibits the characteristic 110 and 020 reflections of the orthorhombic  $\beta$ -structure<sup>4</sup> indicated by thick arrows in Figure 2. However, because of the fact that the  $\beta$ -phase evolves with time toward a monoclinic  $\alpha$ -structure, when PBA is kept at room temperature,<sup>4</sup> some of the traces of the 110 and 020 reflections of the  $\alpha$ -phase, marked by thin arrow in

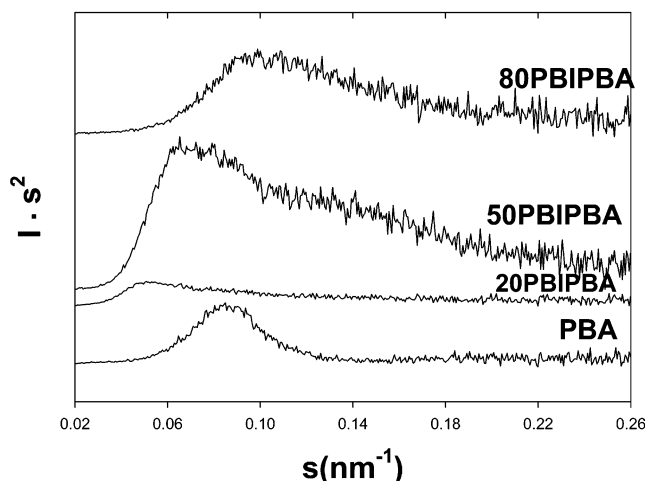


**Figure 3.** SAXS scattered intensity as a function of reciprocal lattice vector for the investigated semicrystalline PBIPBA copolymers.

Figure 2, are detectable in the WAXS pattern of PBA. Indeed, also the 20PBIPBA copolymer presents Bragg peaks characteristic of the both the  $\alpha$ - and  $\beta$ -crystalline phases of PBA although here the presence of PBI units seems to favor the  $\alpha$ -phase structure.

Figure 3 shows the Lorentz-corrected<sup>13</sup> SAXS patterns of the PBA and PBIPBA samples at room temperature. As mentioned above, PBI remains amorphous under these conditions. As expected, all samples exhibit maxima in the Lorentz-corrected scattered intensity, indicating the existence of a lamellar crystal packing. The broadness of the SAXS peaks for the copolymers is characteristic of a broad distribution of lamellar stacks present in specimens with a low level of crystallinity. The broadness decreases significantly for the most crystalline specimen, PBA, as a consequence of the chemical homogeneity. An experimental average periodicity of the distribution of lamellar stacks can be estimated by the long period  $L = 1/s_{\max}$ , where  $s_{\max}$  is the scattering maximum. The values are shown in Table 1 for the different investigated samples. As can be seen, the long period values, starting from PBA, reach a maximum for the 20PBIPBA sample.

### 3.2. Dielectric Loss Spectroscopy Experiments.

To introduce the general relaxation behavior of PBIPBA copolymer, the dielectric loss values,  $\epsilon''$ , measured as a function of temperature and frequency are illustrated in Figure 4 for the completely amorphous as well as semicrystalline ( $X_c^{\text{WAXS}} = 10\%$ ) 50PBIPBA copolymer. In both cases, two main dielectric relaxations regions are evident:  $\beta$  and  $\alpha$  in the order of increasing temperature. The relaxation processes appear as maxima in  $\epsilon''$  vs log frequency moving toward higher temperatures as frequency increases. The more intense  $\alpha$ -process appears above the calorimetric glass transition temperature (see Table 1). For the semicrystalline sample, the peak height of the  $\alpha$ -relaxation is significantly reduced as compared to that of the amorphous one whereas the  $\beta$ -relaxation is slightly affected. Analyzing in detail the  $\beta$ -relaxation region, one can see that it is rather broad and seems to be composed of two processes, designated as  $\beta''$  and  $\beta'$  in order of increasing temperature, which will be described in detail below.

#### 3.2.1. Relaxation of the Amorphous Systems.

##### 3.2.1.a. Low-Temperature Relaxation Processes.

Figure 5 illustrates the dielectric loss ( $\epsilon''$ ) values for both

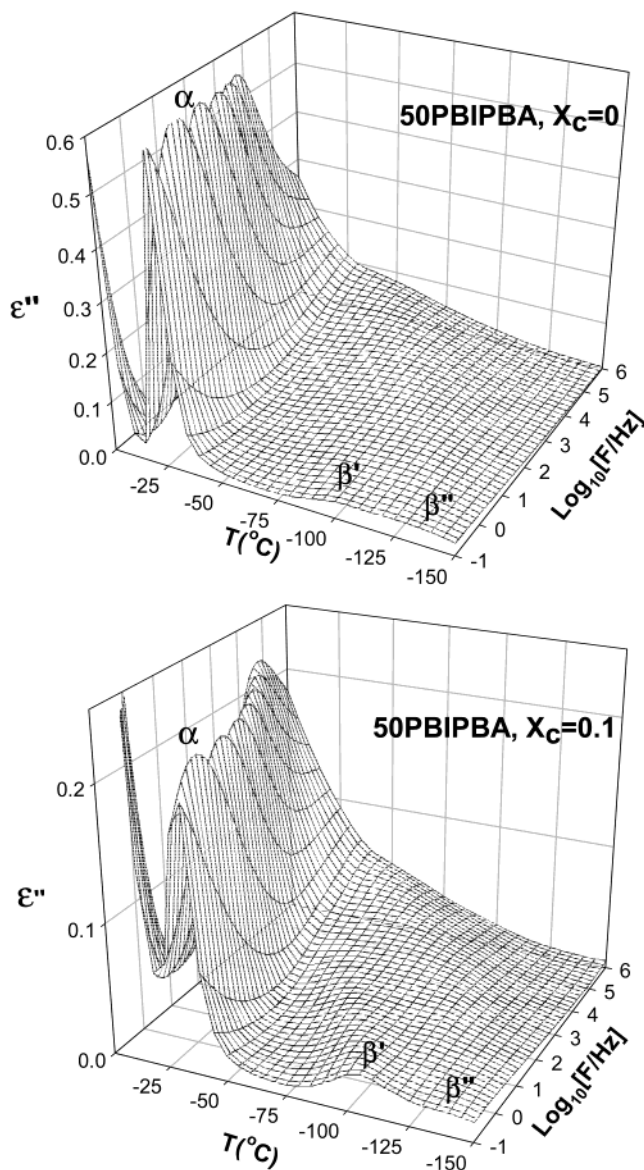


**Figure 4.**  $\epsilon''$  values for the amorphous (top) and semicrystalline  $X_c = 0.1$  50PBIPBA copolymer as a function of frequency and temperature.

$\beta$ -relaxation (left) and  $\alpha$ -relaxation (right) regions, measured for the amorphous samples of PBI, 80PBIPBA, and 50PBIPBA copolymers, as a function of frequency at several temperatures. The PBA and 20PBIPBA samples could not be obtained in an amorphous state by quenching as previously mentioned. For PBI and 80PBIPBA, the  $\beta$ -relaxation process (Figure 5, left) appears as a broad maximum in  $\epsilon''$  moving toward higher frequency as temperature increases. The  $\beta$ -relaxation region for the 50PBIPBA sample consists of two processes denoted hereafter as  $\beta'$  and  $\beta''$  in order of increasing frequency. As temperature increases,  $\beta'$  merges into  $\beta''$ . To estimate the frequency of maximum loss,  $F_{\max}$ , for both contributions, a strategy based on the Coburn and Boyd<sup>1</sup> procedure was followed as explained in the Appendix. The continuous lines in Figure 5 represent the global fits according to a Cole–Cole function (eq 1 with asymmetry parameter  $c = 1$ ). For the 50PBIPBA a sum of two Cole–Cole functions was used to describe the relaxation. Figure 6 shows the frequency of the maximum loss peak,  $F_{\max}$ , as a function of the reciprocal temperature for the low-temperature



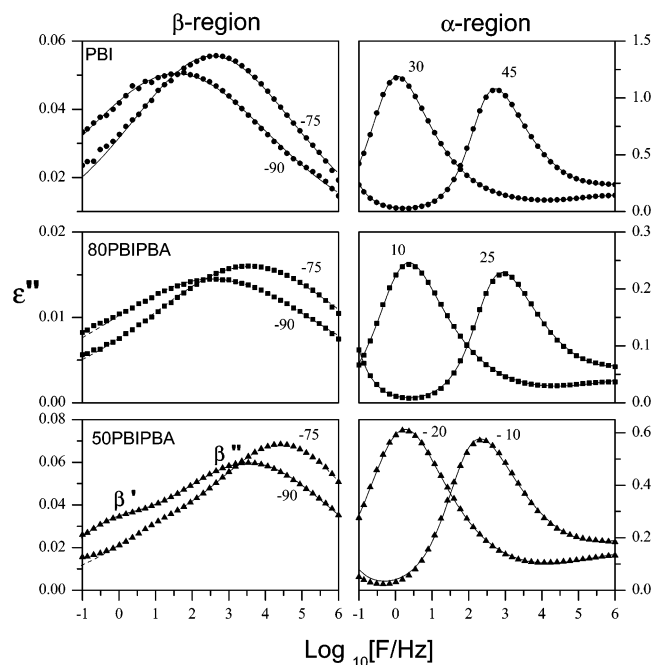


**Figure 5.** Isothermal  $\epsilon''$  data of amorphous PBI, 80PBIPBA, and 50PBIPBA copolymers as a function of frequency for some selected temperatures. Continuous lines represent best fits according to the Cole–Cole equation for the  $\beta$ -processes and HN for the  $\alpha$ -relaxation.

relaxation processes of the amorphous samples (solid symbols). In such a representation, all processes follow an Arrhenius behavior. This is characteristic of subglass relaxation processes.<sup>14</sup> From the slope of the straight line it is possible to obtain the activation energy. Concerning the  $\beta$ -relaxation of PBI and 80PBIPBA and the  $\beta''$  of 50PBIPBA, similar values for the activation energy ( $E_a \approx 44$  kJ mol<sup>-1</sup>) are obtained regardless the composition. A slightly higher value is calculated for the  $\beta'$ -process of 50PBIPBA. The values are consistent with the assignment of this relaxation to the subglass relaxation associated with the ester groups attached to the polymeric chain.<sup>1,14,15</sup> The position of  $F_{\max}$  is significantly affected by the composition. In fact, considering similar temperatures, the  $F_{\max}$  values shift toward higher frequencies as the butylene isophthalate units content decreases. This behavior contrasts with that observed in other copolymeric systems in which both comonomeric units contain aromatic rings. In these cases no dependence of the  $\beta$ -relaxation with molar ratio is observed.<sup>16,17</sup>

**3.2.1.b. Higher Temperature Processes:  $\alpha$ -Relaxation.** Figure 5 (right) illustrates the dielectric loss data in the temperature region  $T > T_g$  for the amorphous copolymers. The  $\alpha$ -relaxation manifests itself as an intense maximum in  $\epsilon''$ , which moves toward higher frequencies as temperature increases. At higher frequencies the less intense contribution of the  $\beta$ -relaxation region is also observed. Additionally, at lower frequencies, a strong increment of  $\epsilon''$ , associated with the electrical conductivity, is also detected. The continuous lines in Figure 5 (right) represent the overall fits according to eq 1 considering two relaxations.<sup>1,18</sup> A detailed description of the fitting strategy is presented in the Appendix. Figure 7 shows the frequency of the maximum loss peak,  $F_{\max}$ , as a function of the reciprocal temperature for the  $\alpha$ -process of the amorphous samples (solid symbols). As is seen, in all cases the  $\alpha$ -process displays a curvature at the higher measured frequencies

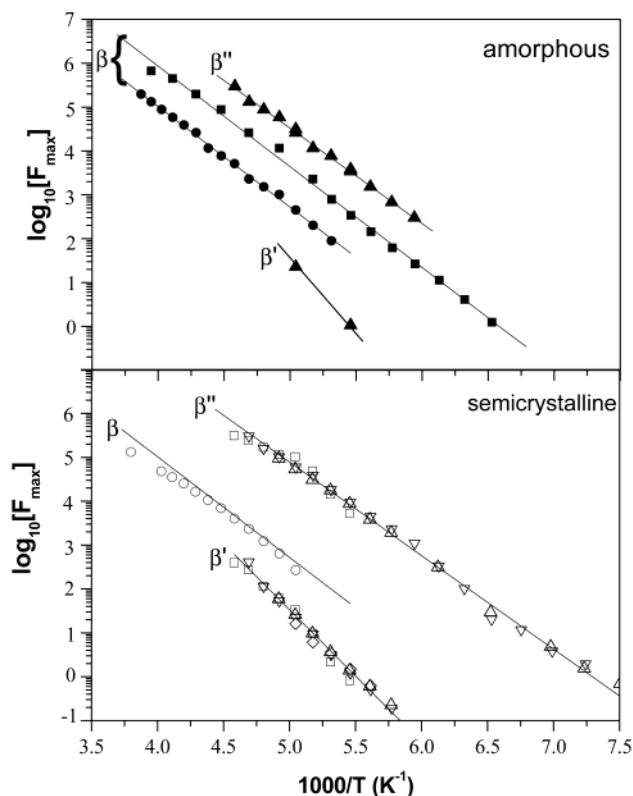


**Figure 6.** Frequency of maximum loss ( $F_{\max}$ ) as a function of reciprocal temperature in the  $\beta$ -relaxation region for the PBIPBA copolymers. Full and hollow symbols represent amorphous (top) and semicrystalline (bottom) specimens, respectively. Continuous lines represent Arrhenius fits for  $\beta'$  and  $\beta''$ . Symbols are as follows: (○, ●) PBI; (□, ■) 80PBIPBA; (△, ▲) 50PBIPBA; (▽) 20PBIPBA; (◇) PBA.

characteristic of a Vogel–Fulcher–Tamman (VFT) dependence:

$$F_{\max} = F_0 \exp \left[ \frac{-DT_0}{T - T_0} \right] \quad (2)$$

where  $F_0$  is a characteristic frequency,  $T_0$  is the Vogel temperature, and  $D$  is the fragility strength parameter.<sup>19</sup> This behavior is characteristic of cooperative segmental motions appearing above the glass transition temperature. To obtain accurate fits, and in accordance with a recent proposal,<sup>20</sup> a value of  $F_0$  of  $1.6 \times 10^{13}$  Hz was assumed. The dashed lines in Figure 7 represent the best fits of the experimental  $F_{\max}$  values to eq 2. The corresponding parameters are collected in Table 2. The obtained values for  $T_0$  decrease with increasing butylene adipate units content as expected on the basis of the progressive increasing of backbone flexibility, also evidenced by the decrease of  $T_g$  as the aliphatic units content increases (Table 1).

### 3.2.2. Relaxation of the Semicrystalline Systems.

#### 3.2.2.a. Low-Temperature Relaxation Processes.

Figure 8 (left) shows  $\epsilon''$  values as a function of frequency in the  $\beta$ -relaxation region at several temperatures for the semicrystalline PBI and PBIPBA copolymers. The crystallinity index values,  $X_c^{\text{WAXS}}$ , as estimated from the WAXS patterns are shown in Table 1. As seen in Figure 8 (left), the dielectric spectra of semicrystalline copolymers are characterized in the low-temperature region by two relaxation processes, labeled as  $\beta'$  and  $\beta''$  in order of increasing frequency. The continuous lines in Figure 8 (left) represent the results of fitting the experimental

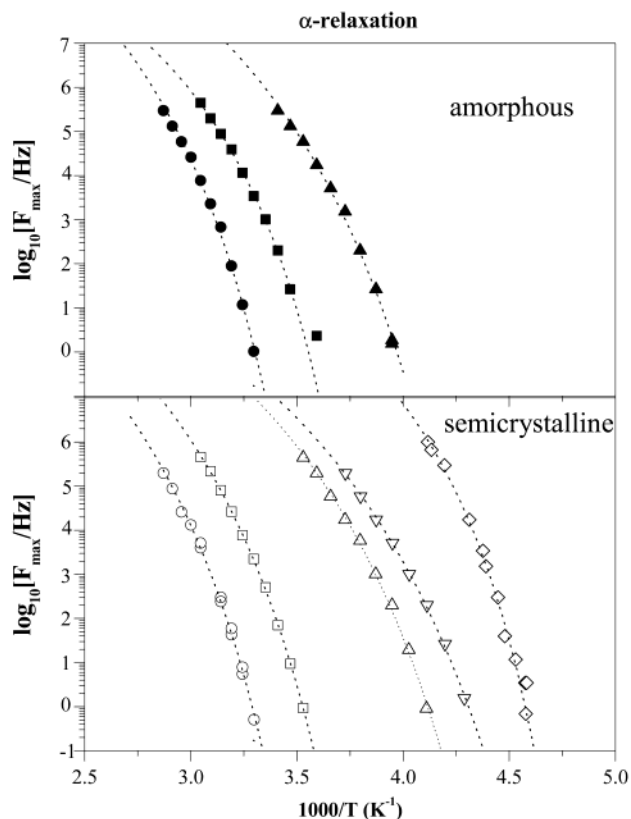


**Figure 7.** Dependence of the frequency of maximum loss ( $F_{\max}$ ) with the reciprocal temperature in the  $\alpha$ -relaxation region for the PBIPBA copolymers. Full and hollow symbols represent amorphous and semicrystalline specimens, respectively. Dashed lines represent Vogel–Fulcher–Tamann fits. Symbols are as follows: ( $\circ$ ,  $\bullet$ ) PBI; ( $\square$ ,  $\blacksquare$ ) 80PBIPBA; ( $\triangle$ ,  $\blacktriangle$ ) 50PBIPBA; ( $\nabla$ ,  $\blacktriangledown$ ) 20PBIPBA; ( $\diamond$ ) PBA.

**Table 2.** Vogel–Fulcher–Tamman Parameters for  $\alpha$ -Relaxation of Amorphous and Semicrystalline PBIPBA Copolymers

BI/BA	$D$	$T_0$ (K)
<b>Amorphous Samples</b>		
100/0 (PBI)	8.1	238.8
80/20	8.5	218.5
50/50	8.3	197.2
<b>Semicrystalline Samples</b>		
100/0 (PBI)	7.8	242.3
80/20	8.0	224.5
50/50	8.0	191.5
20/80	8.8	179.2
0/100 (PBA)	4.7	188.5

data to eq 1 considering two symmetric relaxations ( $c = 1$ ). The corresponding fitting parameters are shown in the Appendix. It is observed that the  $\beta''$ -relaxation for the semicrystalline 80PBIPBA and 50PBIPBA copolymers tends to be enhanced as compared to that of the corresponding amorphous samples (Figure 5, left). Figure 9 shows  $\epsilon''$  values for the semicrystalline PBA in an isochronal fashion. In this case, the low intensity of  $\epsilon''$  data prevents a frequency-resolved analysis. However, for the two selected frequencies the low-temperature relaxation process is clearly detected. It is to be remarked that while semicrystalline PBIPBA copolymers exhibit two low-temperature relaxations semicrystalline PBI and PBA exhibit a single one. The  $F_{\max}$  values for the low-temperature processes observed in the semicrystalline PBIPBA copolymers are included in Figure 6 as a function of reciprocal temperature (open

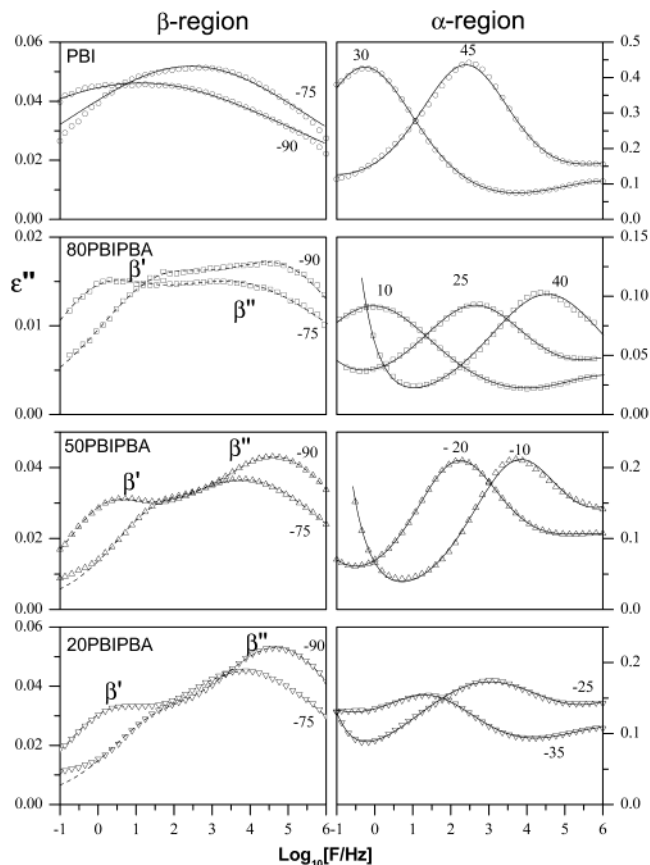


**Figure 8.** Isothermal  $\epsilon''$  data of semicrystalline PBI, 80PBIPBA, 50PBIPBA, and 20PBIPBA copolymers as a function of frequency for some selected temperatures. Continuous lines represent best fits according to Cole–Cole equation for the  $\beta$ -processes and HN for the  $\alpha$ -relaxation.

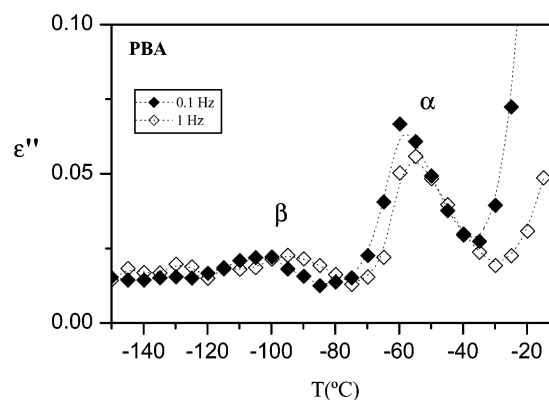


**Figure 9.** Isochronal  $\epsilon''$  data for semicrystalline PBA at 0.1 Hz (full symbol) and 1 Hz (hollow symbol).

symbols). As one sees, in all cases the Arrhenius behavior is followed, and the activation energies obtained are around 41 and 58  $\text{kJ mol}^{-1}$  for  $\beta''$  and  $\beta'$ , respectively. These values are in agreement with those reported for subglass relaxation of ester groups.<sup>14,15</sup> It is observed that  $F_{\max}$  values corresponding to the  $\beta$ -relaxation in amorphous and semicrystalline specimens of PBI are similar regardless of crystallinity. On the contrary,  $F_{\max}$  values for the copolymers are significantly affected by crystallinity. For example, at constant temperature, the presence of crystallinity causes a significant shift of the  $\beta''$ -relaxation  $F_{\max}$  values toward higher frequencies in the case of 80PBIPBA and 50PBIPBA copolymers. On the contrary,  $F_{\max}$  values associ-

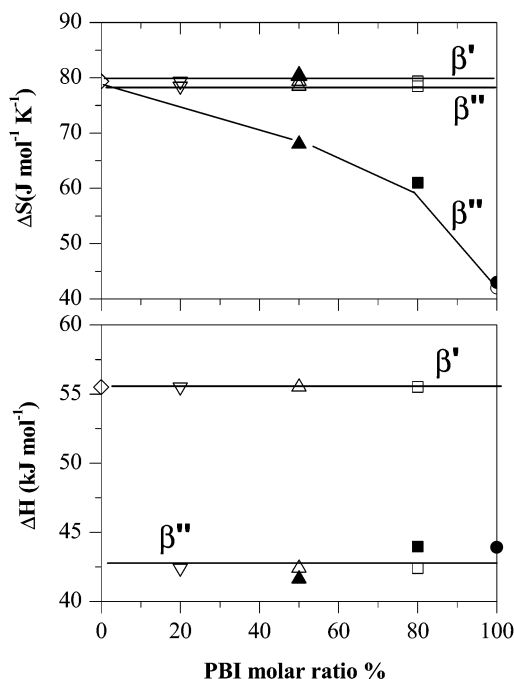


**Figure 10.** Entropy (top) and enthalpy (bottom) values estimated from the Eyring equation for the amorphous (full symbols) and semicrystalline (hollow symbols) copolymers as a function of the BI molar ratio. Symbols are as follows: (○, ●) PBI; (□, ■) 80PBIPBA; (△, ▲) 50PBIPBA; (▽) 20PBIPBA; (◇) PBA.

ated with the  $\beta'$ -relaxation do not exhibit any remarkable dependence with the molar ratio and appear located nearly at the same position as that of PBA.

**3.2.2.b. Higher Temperature Relaxation Process.** Figure 8 (right) illustrates the  $\epsilon''$  values as a function of frequency in the  $T > T_g$  temperature region for the PBI and PBIPBA copolymers. In all cases, the peak height of the relaxation is comparatively weaker than that of the amorphous ones. This is a result of the expected reduction of the amorphous relaxing fraction.<sup>1,2,21</sup> Similar to the amorphous samples, the semicrystalline copolymers show a main  $\alpha$ -relaxation and a less intense contribution of the  $\beta$ -relaxation at high frequencies. At low frequencies, a conductivity contribution is also detected. The continuous solid lines in Figure 8 (right) represent the results of fitting the experimental data with the eq 1 considering two relaxation processes. The corresponding fitting parameters are presented in the Appendix and in Figure 12. It is seen that the crystallinity has a dramatic influence on the shape of the  $\alpha$ -relaxation, especially for the semicrystalline 80PBIPBA and 50PBIPBA copolymers. Here, a significant reduction of the asymmetry of the relaxation process is detected by an increase of the  $c$  parameter from  $\approx 0.4$  to 1 and an increase of the broadening, as revealed by the reduction of the  $b$  parameter from  $\approx 0.9$  to 0.4. The reduction of the asymmetry of the overall  $\alpha$ -relaxation for the semicrystalline specimens suggests the presence of two processes. One occurring in a unrestricted amorphous phase, contributing to the higher frequency part of the spectrum, and a second perturbed  $\alpha$ -process affected by the crystalline phase influencing the lower frequency tail of the relaxation. It must be emphasized that dielectric measurements clearly detect the broadening at low frequencies, in agreement with previous observations.<sup>1-3,21,22</sup> Thus, dielectric measurements are sensitive to the effects of

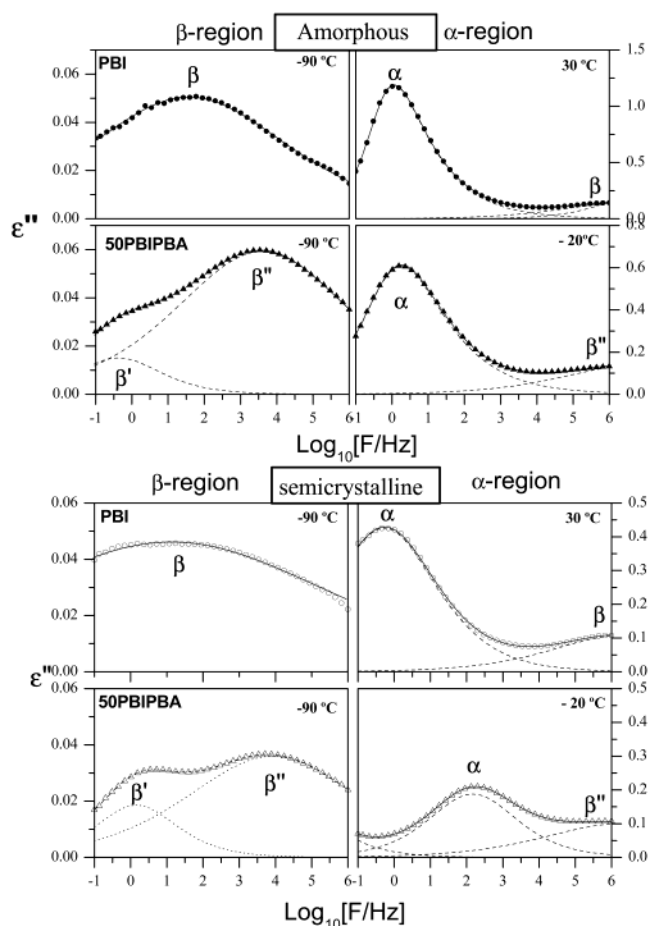


**Figure 11.** Isothermal  $\epsilon''$  vs frequency for PBI and 50PBIPBA at selected temperatures for amorphous (top, full symbols) and semicrystalline (bottom, hollow symbols) specimens. Dashed lines show the separated contribution of the different relaxation processes. Symbols are as follows: (○, ●) PBI; (△, ▲) 50PBIPBA.

the crystalline phase on the adjacent amorphous regions, effects which are proven by NMR only after complicate analyses limited in frequency range. In addition, the  $\alpha$ -relaxation of semicrystalline 50PBIPBA copolymer shows a strong shift of the  $F_{\text{max}}$  position toward higher frequencies. This behavior is anomalous since the presence of crystalline regions usually restricts the cooperative segmental motions related to this relaxation.<sup>1,2,21</sup> The frequencies of the maximum loss peak values,  $F_{\text{max}}$ , for the  $\alpha$ -process of the semicrystalline copolymers are represented by the open symbols in Figure 7 as a function of the reciprocal temperature. As is seen, the  $\alpha$ -process for the semicrystalline samples displays a curvature at the higher measured frequencies characteristic of a Vogel–Fulcher–Tamman (VFT) dependence. The dashed lines in Figure 7 represent the best fits of the experimental  $F_{\text{max}}$  values to the VFT equation. The corresponding parameters are collected in Table 2. It is noteworthy that the semicrystalline PBI and 80PBIPBA exhibit a VFT behavior very close to that of the corresponding amorphous samples. On the contrary, a shift of the  $F_{\text{max}}$  position toward lower temperatures is observed in the case of semicrystalline 50PBIPBA copolymer in comparison to the amorphous sample. As mentioned above, this implies an anomalous enhanced segmental mobility induced by the crystalline phase. Such an effect will be discussed in the forthcoming paragraphs.

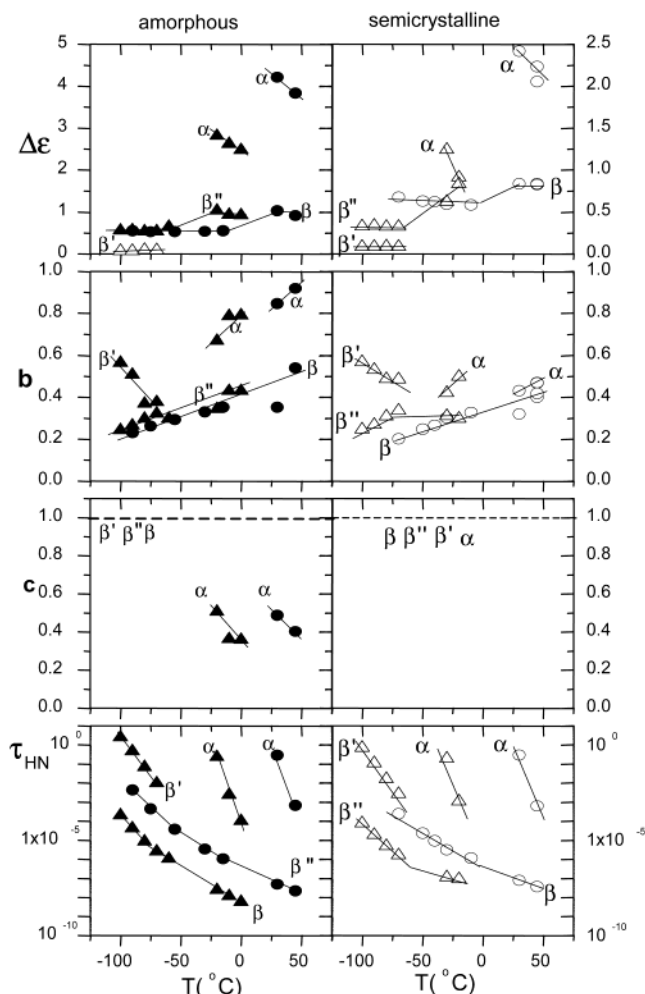


**Figure 12.** Dielectric strength  $\Delta\epsilon$ , shape parameters  $b$  and  $c$ , and central relaxation time  $\tau_{HN}$  corresponding to the HN analysis of the dielectric data for amorphous (left, full symbols) and semicrystalline (right, hollow symbols) systems. Symbols are as follows: (○, ●) PBI; (Δ, ▲) 50PBIPBA.

#### 4. Discussion

**4.1. Structure Development.** The X-ray scattering experiments show that a crystalline structure develops in the PBIPBA copolymers by appropriated heat treatment. The WAXS patterns indicate that the dominating crystal phase is to be related to the lattice of the PBI homopolymer, as supported by the presence of the most intense Bragg Peaks, around  $s = 0.19$  and  $0.27 \text{ \AA}^{-1}$ , characteristic of PBI.<sup>5</sup> The predominant presence of the PBI crystal phase in these copolymers may be surprising taking into account the difficulty of the PBI homopolymer to crystallize in comparison with PBA but can be understood by considering the close connection between the dynamical behavior and the molar ratio. PBIPBA random copolymers possess higher flexibility in comparison with original PBI. We can hypothesize that the increment in chain flexibility of the copolymer increases the facility of PBI segments to find a crystalline register. The SAXS spectra show the existence of a crystalline lamellar packing with an average periodicity given by the long period values. As is shown in Table 1, the long spacing values tend to reach a maximum value for the 20PBIPBA copolymer. This trend correlates well with the melting point dependence on molar ratio which also exhibits a minimum between 20PBIPBA and 40PBIPBA,<sup>7</sup> suggesting that for a given composition the less

abundant comonomeric units tend to hinder the crystallization of the most abundant one, leading to lamellae with smaller and more disperse crystals.<sup>6-8</sup>

**4.2. Subglass Relaxation Behavior.** The  $\beta$ -relaxation region observed in the PBIPBA copolymers can be ascribed to subglass motions in the amorphous phase.<sup>1,14,15</sup> As seen from Figures 5 and 8 (left), the  $\beta$ -relaxation region is affected by both composition and crystallinity. While the dielectric spectrum of PBI is characterized by a single  $\beta$  process which is essentially unaffected by the crystallinity, those of the copolymers exhibit an additional lower frequency process which becomes more evident as the amount of butylene adipate content increases. This process, although evident at  $-90^\circ\text{C}$  for the 50PBIPBA amorphous system (Figure 5, left), is even clearer for the semicrystalline 80PBIPBA, 50PBIPBA, and 20PBIPBA copolymers. These samples exhibit two low-temperature processes,  $\beta'$  and  $\beta''$ , in order of increasing frequency (Figure 8, left). From inspection of Figure 6, one sees that  $F_{\max}$  values for the  $\beta'$ -relaxation are located within the range of the  $\beta$ -relaxation of the PBA homopolymer and present similar activation energies. Consequently, we can attempt to ascribe such  $\beta'$ -relaxation to the ester group motions of the butylene adipate comonomeric units. As the dominating crystal phase is that of PBI, it is expected that the amorphous phase of the copolymer becomes enriched in butylene adipate counts. Accordingly, the  $\beta'$ -relaxation becomes more evident in the semicrystalline specimens. By looking at the  $F_{\max}$  values represented in Figure 6, one sees that the  $\beta''$ -relaxation  $F_{\max}$  values of the amorphous specimens shift, for similar temperatures, toward higher frequencies as the butylene adipate content increases. On the contrary, the corresponding values for the semicrystalline specimens lay on the same line regardless of molar ratio. The shift of the  $\beta''$ -relaxation  $F_{\max}$  values exhibited by the amorphous specimens indicates an enhancement of the mobility with increasing butylene adipate content. Such a trend is unexpected since the  $\beta''$ -relaxation is related to noncooperative motions, and therefore the  $F_{\max}$  position should be slightly dependent on the environment. An extension of the Arrhenius equation is given by Eyring,<sup>23</sup> which proposes for  $F_{\max}$

$$F_{\max} = (kT/2\pi h) \exp(\Delta S/k) \exp(-\Delta H/kT) \quad (3)$$

where  $\Delta S$  and  $\Delta H$  are the molar entropy and enthalpy of activation, respectively, and  $h$  and  $k$  are the Planck and Boltzmann constants, respectively. According to eq 3, the entropic exponential factor may shift the relaxation straight lines parallel to the reciprocal temperature axis depending on the values of  $\Delta S$ . We have estimated the  $\Delta S$  values by introducing the calculated value for the activation energy as  $\Delta H$  in eq 3. The calculated values for  $\Delta H$  and  $\Delta S$  values are reported in Figure 10 as a function of butylene isophthalate content for amorphous and semicrystalline copolymers. For the semicrystalline copolymers the  $\Delta H$  and  $\Delta S$  values concerning the  $\beta'$ -relaxation are similar to those for PBA homopolymer further, supporting the assignment of the  $\beta'$ -relaxation to the butylene adipate counts. It can be observed that both the amorphous and semicrystalline systems exhibit similar  $\beta''$ -relaxation  $\Delta H$  values whereas the  $\Delta S$  values depends on composition and crystallinity. Previous studies on poly(ethylene terephthalate) and poly(ethylene isophthalate) copolymers<sup>16</sup> support the hypothesis that the motion associated with the  $\beta$ -relax-



ation is restricted to the molecular structure between consecutive phenyl rings. Therefore, one may assume that the subglass motion in PBI is also damped by consecutive phenyl rings and therefore restricted to the single monomer. The molecular structure of PBA is similar to the moiety located between consecutive phenyl rings in PBI (Figure 1). Upon increasing the butylene adipate segments, the probability of finding several similar moieties between two phenylene rings continuously increases. This implies that the possible damping of the motion should decrease with increasing butylene adipate content. Consequently, the molecular motion responsible for the  $\beta''$ -relaxation could increasingly spread out along the chain with increasing butylene adipate content, causing an enhancement of the intrachain cooperativity of the subglass relaxation. As more "disorder" would be involved by this effect, a progressive increase of  $\Delta S$  would be expected. However, for the semicrystalline specimens, this effect in the  $\beta''$ -relaxation is only seen upon comparing PBI and the copolymers but not among the copolymers themselves. In fact, similar  $\Delta H$  and  $\Delta S$  values were estimated from eq 3 for semicrystalline copolymers regardless of molar ratio. As estimated from WAXS, crystallinity tends to increase with increasing butylene adipate content (Table 1). The presence of crystals, which act as physical cross-links, can be responsible for an increase in the damping of the subglass motions counterbalancing the enhanced mobility imparted by the aliphatic units. In fact, this effect is known for the cooperative  $\alpha$ -relaxation,<sup>1,2,21</sup> but it is unusual for subglass relaxations.

**4.3. Segmental Dynamics.** The  $\alpha$ -relaxation observed in the PBIPBA copolymers can be ascribed to segmental motions in the amorphous phase which appear above the glass transition temperature. As it seen from Figures 5 and 8 (right), the  $\alpha$ -relaxation is affected by both composition and crystallinity. By looking at the  $F_{\max}$  values represented in Figure 7, one sees that the  $\alpha$ -relaxation  $F_{\max}$  values for the amorphous specimens shift, for similar temperature, toward higher frequencies as the butylene adipate units content increases. This is a consequence of the progressive increase in chain flexibility as the amount of aliphatic units increases.<sup>8,24</sup> More surprising in these copolymers is the influence of crystallinity on the segmental dynamics. As is shown in Figures 5 and 8 (right), the  $\alpha$ -relaxation for semicrystalline PBI and for the 80PBI-PBA copolymer appears at lower frequencies as compared with that of the amorphous sample. This is a consequence of the characteristic slowing down of the amorphous phase segmental dynamics induced by the crystalline phase.<sup>1,2,21,25</sup> However, in the case of the 50PBIPBA copolymer, the  $\alpha$ -relaxation for the semicrystalline sample appears at a frequency which is about 2 orders of magnitude faster than that of the corresponding amorphous specimen. This is an anomalous effect considering that segments located in the amorphous phase are pinned at the crystal surface, and the amorphous phase dynamics should be slowed down as a consequence of increasing intramolecular cooperativity.<sup>26,27</sup> The diffraction pattern of 50PBIPBA copolymer (Figure 2) resembles closely that of the PBI homopolymer, suggesting that the crystalline phase developed in the 50PBIPBA copolymer is that of PBI. Consequently, it is expected that the molar ratio of the amorphous phase is being progressively enriched in the butylene adipate comonomeric units during crystallization. PBA

is more flexible than PBI and therefore is characterized by an  $\alpha$ -relaxation process appearing at lower temperatures. Therefore, the anomalous dynamic behavior observed in the 50PBIPBA semicrystalline copolymer can be explained as due to an enrichment of the amorphous phase in the more flexible butylene adipate comonomeric units.

## 5. Conclusions

In conclusion, the introduction of flexible butylene adipate units into the more rigid PBI chain increases the ability to crystallize at room temperature of the resulting copolymer. X-ray scattering experiments indicate that the dominating crystal phase is related to the lattice characteristic of the butylene isophthalate units. The subglass dynamics of PBIPBA copolymers is characterized by the existence of two processes,  $\beta'$  and  $\beta''$ , which become more evident in the semicrystalline specimens and have been assigned to the relaxation of the individual butylene adipate and butylene isophthalate comonomeric units, respectively. The unexpected enhanced mobility in the case of the  $\beta''$ -relaxation with increasing butylene adipate content for the amorphous specimens has been discussed by considering a progressive increase of the intrachain cooperativity. The segmental dynamics of these copolymers is characterized by the existence of an  $\alpha$ -relaxation which, for the amorphous specimens, follows an expected molar ratio behavior. However, an anomalous enhanced mobility is observed in the semicrystalline 50PBIPBA copolymer. This effect has been explained by considering the progressive enrichment of the amorphous phase in butylene adipate segments as crystallinity develops. Our results seem to indicate that by copolymerizing appropriated aromatic esters with aliphatic ones of higher flexibility it is possible to obtain semicrystalline polymeric systems in which the characteristic dynamical retardation of the amorphous phase upon crystallization could be not only precluded but even enhanced.

**Acknowledgment.** C. Alvarez gratefully acknowledges the tenure of a fellowship awarded by the Comunidad de Madrid. The authors thank the financial support from the MCYT (Grant FPA2001-2139), Spain, for generous support of this investigation. The experiments at HASYLAB (Hamburg, Germany) have been funded by the IHP-Contract HPRI-CT-1999-00040 of the European Commission (EC(ERBFMGEDT 950059) and II-00-015 EC).

## Appendix. Fitting Strategy

As mentioned in the Results section, eq 1 was used in order to estimate the values of the frequency of maximum loss,  $F_{\max}$ , presented in Figures 5 and 8. The shape parameters characterizing the dielectric relaxation were obtained following an extrapolation procedure based on that proposed by Coburn and Boyd.<sup>1</sup> To estimate the accuracy of the fitting parameters, their values have been varied. We found that the maximum possible variation without provoking a significant deviation between the measured and calculated curves was less than  $\pm 5\%$  for  $b$ ,  $c$ , and  $\Delta\epsilon$  and  $\pm 10\%$  for  $\tau_{\text{HN}}$ . In this appendix we include as an example the procedure followed for the PBI homopolymer and for the 50PBI-PBA copolymer. In the case of the amorphous samples, Figure 11 shows the experimental data obtained for the  $\beta$ -relaxation region (left) and for the  $\alpha$ -relaxation (right)



at those temperatures for which the relaxation is well on the experimental frequency window. Similarly, experimental data for the semicrystalline samples are shown in Figure 11. In the  $\beta$ -region, the continuous lines correspond to the best fit using a single or a double Cole–Cole function (eq 1 with  $c = 1$ ) for PBI and 50PBIPBA, respectively. In the last case, the dashed lines represent the individual components, labeled as  $\beta'$  and  $\beta''$  in order of increasing frequency. The corresponding HN parameters are presented in Figure 12 as a function of temperature. As is seen in this figure,  $\Delta\epsilon$  and  $b$  follow linear variations with temperature. As temperature increases, the  $\beta'$  merges into the  $\beta''$ , giving rise to a single relaxation whose  $F_{\max}$  values follows Arrhenius behavior. In the  $\alpha$ -relaxation region (see Figure 11 (right)) a HN function for the  $\alpha$ -process and a Cole–Cole function for the  $\beta$ -process were used to fit the data. The dashed lines indicate the individual components. Shape parameters are presented in Figure 12. To limit the number of parameters, the  $\tau_{\text{HN}}$  values were extrapolated assuming an Arrhenius dependence of the low-temperature data.<sup>1,18</sup>

## References and Notes

- (1) Coburn, J. C.; Boyd, R. H. *Macromolecules* **1986**, *19*, 2238.
- (2) Williams, G. *Adv. Polym. Sci.* **1979**, *33*, 59.
- (3) Nogales, A.; Ezquerro, T. A.; García, J. M.; Baltá-Calleja, F. *J. Polym. Sci., Part B: Polym. Phys.* **1999**, *37*, 37.
- (4) Minke, R.; Blackwell, J. *J. Macromol. Sci., Phys.* **1979**, *B16*, 407.
- (5) Phillips, R. A.; McKenna, J. M.; Cooper, S. L. *J. Polym. Sci., Part B: Polym. Phys.* **1994**, *32*, 791.
- (6) Righetti, M. C.; Pizzoli, M.; Lotti, N.; Munari, A. *Macromol. Chem. Phys.* **1998**, *199*, 2063.
- (7) Righetti, M. C.; Pizzoli, M.; Munari, A. *Macromol. Chem. Phys.* **1994**, *195*, 2039.
- (8) Munari, A.; Manaresi, P.; Chiorboli, E.; Chiolle, A. *Eur. Polym. J.* **1992**, *28*, 101.
- (9) Šics, I.; Ezquerro, T. A.; Nogales, A.; Baltá-Calleja, F. J.; Kainins, M.; Tupureina, V. *Biomacromolecules* **2001**, *2*, 581.
- (10) Havriliak, S.; Negami, S. *Polymer* **1967**, *8*, 161.
- (11) Kirst, K. U.; Kremer, F.; Litinov, V. M. *Macromolecules* **1993**, *26*, 975.
- (12) Blundell, D. J.; Osborn, B. N. *Polymer* **1983**, *24*, 953.
- (13) Baltá-Calleja, F. J.; Vonk, G. G. *X-ray Scattering of Synthetic Polymers*; Elsevier Science: New York, 1989.
- (14) McCrum, N. G.; Read, B. E.; Williams, G. *Anelastic and Dielectric Effects in Polymeric Solids*; Dover: New York, 1991.
- (15) Hedvig, P. *Dielectric Spectroscopy of Polymers*; Adam Hilger Ltd.: Bristol, 1977.
- (16) Tatsumi, T.; Ito, E.; Hayakawa, R. *J. Polym. Sci., Part B: Polym. Phys.* **1992**, *30*, 701.
- (17) Ezquerro, T. A.; Baltá-Calleja, F. J.; Zachmann, H. G. *Acta Polym.* **1993**, *44*, 18.
- (18) Nogales, A.; Denchev, Z.; Šics, I.; Ezquerro, T. A. *Macromolecules* **2000**, *33*, 9367.
- (19) Richert, R.; Angell, C. A. *J. Chem. Phys.* **1998**, *21*, 9016.
- (20) Angell, C. A. *Polymer* **1997**, *38*, 6261.
- (21) Ezquerro, T. A.; Majszczyk, J.; Baltá-Calleja, F. J.; López-Cabarcos, E.; Gardner, K. H.; Hsiao, B. S. *Phys. Rev. B* **1994**, *50*, 6023.
- (22) Hensel, A.; Dobbertin, J.; Schawe, J. E. K.; Boller, A.; Schick, A. *J. Therm. Anal.* **1996**, *46*, 935.
- (23) Blythe, A. R. *Electrical Properties of Polymers*; Cambridge University Press: Cambridge, 1980.
- (24) Couchman, P. R. *Macromolecules* **1987**, *20*, 223.
- (25) Fukao, K.; Miyamoto, Y. *Phys. Rev. Lett.* **1997**, *79*, 4613.
- (26) Ngai, K. L.; Roland, C. M. *Macromolecules* **1993**, *26*, 2688.
- (27) Roland, C. M. *Macromolecules* **1994**, *27*, 4242.

MA025993V